Electron-electron interaction and the persistent current in a quantum ring

Tapash Chakraborty*
Institute of Mathematical Sciences, Taramani, Madras 600 113, India

Pekka Pietiläinen†
Department of Theoretical Physics, University of Oulu, Linnanmaa, SF-90570 Oulu 57, Finland
(Received 23 March 1994)

We have studied the effect of electron-electron interaction on the magnetic moment (associated with the persistent current) of electrons in a quantum ring. We have introduced a model where the electron makes a circular motion in a parabolic confinement simulating a quantum ring which is subjected to a perpendicular magnetic field. The electron states in such a ring with and without the Coulomb interaction are then investigated. We have also explored the limits of narrow and wide rings. Our detailed calculations of the energy spectrum where the interelectron interactions are also included indicate that when the electrons occupy the states of only the lowest Landau band, the interaction merely shifts the spectrum to higher energy and its effect on magnetization is insignificant. The result can be understood as entirely due to conservation of the angular momentum. A qualitative estimate for a large system where electrons also occupy higher Landau bands indicates that the Coulomb interaction mixes some of the states resulting in a rapid increase in the magnetization.

I. INTRODUCTION

A metallic ring of mesoscopic dimension in an external magnetic field is known to exhibit a wide variety of interesting physical phenomena: For example, it can carry an equilibrium current (the so-called persistent current) (Refs. 1–3) which is periodic in the Aharonov-Bohm[4] flux Φ with a period $\Phi_0=hc/e$, the flux quantum. The effect is a direct consequence of the properties of the eigenfunctions of isolated rings, which cause the periodicity of all physical quantities. The reason for this behavior is well known,[5–9] and briefly is as follows: In the case of a ring which encloses a magnetic flux Φ, the vector potential can be eliminated from the Schrödinger equation by introducing a gauge transformation. The result is that the boundary condition is modified as $\psi_n(x+L)=e^{2\pi i\Phi/\Phi_0}\psi_n(x)$, where L is the ring circumference. The situation is then analogous to the one-dimensional Bloch problem with the Bloch wave vector[7–9] $k_n=(2\pi/L)\Phi/\Phi_0$. The energy levels E_n and other related physical quantities are therefore periodic in Φ_0. For a time-independent flux Φ, the equilibrium current (at $T=0$) associated with state n is

$$I_n=-\frac{ev_n}{L}=-c\frac{\partial E_n}{\partial\Phi}\ , \tag{1}$$

where $v_n=\partial E_n/\hbar\partial k_n=(Lc/e)\partial E_n/\partial\Phi$ is the velocity of state n. An important condition for I_n to be nonzero is that the wave functions of the charge carriers should stay coherent along the circumference L of the ring.

It should be pointed out that the persistent current defined above is *not* a transport current, but rather an equilibrium property of the ring which at $T=0$ is directly related to the ground-state energy. It is interesting to recall that the ring geometry and the thermodynamic current (1) played a central role in the gauge-invariance interpretation of the integer quantum Hall effect and the current-carrying edge states.[10–12] Such currents have been detected in recent experiments in an ensemble of $\sim 10^7$ Cu rings,[1] in three single gold rings,[2] and in a single loop (of diameter 2.7 μm) created in a GaAs heterostructure.[3] In the first experiment, the current was found to be periodic in Φ with a period $\frac{1}{2}\Phi_0$, while in the other two experiments the current is also periodic in Φ but the period is Φ_0. The single-ring experiments are more interesting, because there one can avoid the problem of averaging the observed current over a large number of rings—which has been a major topic of discussions in most theoretical work—and a more direct theory like the one presented below is applicable. Rings prepared in semiconductor systems are even more useful for our studies than those made out of pure metals. In fact, mesoscopic rings made in GaAs heterostructures with smaller numbers of electrons (but of higher mobility) are supposed to be the best systems to measure the persistent currents.[13] Experiments on persistent current in a single loop created in the GaAs heterojunction have been reported only recently.[3] Here the disorder is very weak and the carrier density is very low, indicating that the electron-electron interaction should be more important than in a metallic ring. The surprising result is that the electron-electron interaction does not significantly change the value of the persistent current. The aim of our present work, to be described below, is therefore to find out to what extent interelectron interactions influence the persistent current.

It is interesting to note that periodic oscillations of thermodynamic quantities like magnetization as a function of magnetic flux in a *ring topology* have also been known from early theoretical work on the edge states in a circular disk in a strong magnetic field,[14] and from much

earlier work on a thin metallic cylinder in a weak magnetic field,[15] such that $l_0 > r_0$. Here $l_0 \equiv (\hbar c/eB)^{1/2}$ is the magnetic length and r_0 is the radius of the cylinder. The essential contribution to the oscillations was found to be due to the magnetic surface levels corresponding to electrons localized in a narrow layer near the cylinder surface. One other important work in ring geometry is by Wohlleben *et al.*[16] who showed that in the ballistic regime a mesoscopic ring will make a transition from a high-temperature state with no current to a low-temperature state with a persistent current even in the absence of an external field. Finally, we should add in this context that the magnetic properties of the recently discovered graphite needles, often referred to as carbon nanotubes,[17] are also quite intriguing.[18]

Studies of quantum-confined systems, in particular quasi-zero-dimensional electron systems (quantum dots), have received considerable attention in recent years.[19–27] The electrostatic confinement of the two-dimensional electron gas is done by a variety of techniques, and the confinement potential is to a good approximation parabolic. Most of the experimental information about the electron states in these systems has been obtained from far-infrared magnetospectroscopy[22] and magnetocapacitance[27] studies. A theoretical understanding[19,26] of the electronic states of these "artificial atoms"[19,20] is also emerging. In addition, very interesting transport measurements were recently performed by McEuen *et al.*[23] in a semiconductor quantum dot. These authors showed that in the quantum Hall regime the conductance peak has a periodic structure as a function of the magnetic field. The oscillations were explained as due to the magnetic depopulation of the higher Landau levels. From this result, and assuming a constant Coulomb energy, they were able to map out the single-particle energy spectrum,[28] and found it to be in very good agreement with what one expects in a parabolic confinement, studied over half a century ago.[29] Single-electron capacitance spectroscopy[27] is also quite unique in obtaining the energy spectrum of few-electron quantum dots, in particular the spin transitions predicted earlier.[30,31]

In a recent paper, Beenakker, van Houten, and Staring[25] suggested that when the electrons in a disk are in the lowest Landau level and when the charging energy (electrostatic energy associated with the incremental charging of the dot by single electrons) is comparable to the cyclotron energy, the magnetoconductance oscillations are suppressed [Coulomb blockade of the Aharonov-Bohm (AB) effect]. The blockade is lifted and the AB effect is recovered if one considers a quantum ring instead. In semiconductor nanostructures, quantum rings can be created from a two-dimensional electron system with an additional gate within the gates shaping the disk (quantum dot). Application of a negative voltage to this additional gate would deplete the central region of the disk, thereby forming a ring. In the lowest Landau level the basic difference between the two systems is the behavior of the electrochemical potential (or the energy cost associated with the addition of a single electron to the disk or the ring) as a function of the magnetic field which determines the conductance oscillations. The situation is different when the second Landau level is occupied, in which case the electrochemical potential for a dot has the same sawtooth behavior as that for a ring, and the Coulomb blockade of the AB effect, as discussed above, is lifted.[25]

In all of these studies of the ring the effect of the electron-electron interaction has been ignored. This effect is quite important in understanding recent experiments[23,24,27] on mesoscopic systems which, in turn, reflect the behavior of the energy levels. For an ensemble of normal metal rings, electron-electron interaction has indeed been shown to contribute significantly to the persistent current.[32] These studies involve Hartree-Fock or Hartree (for a single ring) (Ref. 33) calculations. In the light of recent experiments on a single mesoscopic ring,[1,2] the effect of electron-electron interaction on the magnetization of electrons in a quantum ring has become an important issue which needs to be understood.

The purpose of this paper is to report on effects of interelectron interaction on the energy spectrum and the magnetic moment associated with the persistent current in a quantum ring.[34] The outline of our paper is as follows. In Sec. II A, we introduce the model Hamiltonian for our quantum ring and present the single-electron formalism. We then show that the earlier results in Refs. 7 and 8 for the metallic ring hold only for the ideal case of a δ-function confinement in our more general scheme.[35] The expression for the interaction matrix elements used in our numerical calculations is derived in detail in Sec. II B and the form used for the magnetization calculation is discussed in Sec. II C. In Sec. III, we present results for the quantum rings of various width. The present study of the Coulomb-interaction effect involves solving numerically the electron states for 4–12 electrons in a quantum ring with parabolic confinement. The accuracy of the method was already very well established in earlier literature.[12,19,26] Our earlier work on quantum dots indicated that, for up to four electrons per dot, Coulomb interaction introduces sawtooth structures in the magnetization curves which are otherwise featureless.[30] These few-electron systems can be taken as the atomic limit of low-dimensional electron systems where the electron screening is not very efficient. In the case of quantum dots, this limit has indeed been achieved in recent experiments,[36] where incremental occupation of the dots with $n_e = 1$, 2, 3, and 4 electrons has been observed. In Sec. III B we then discuss some qualitative results for a 12-electron system. We should finally mention that, since our primary concern is the role of electron-electron interaction on the magnetic moments, here we consider the quantum ring to be free of any impurities. Although the role of disorder in a mesoscopic ring is a widely studied (and yet unclear) topic, our study of the impurity-free system can be justified for a mesoscopic ring created in a semiconductor heterojunction (as in Ref. 3), where the electron motion can be made ballistic.[37]

II. QUANTUM RING MODEL

In our model for the quantum ring the electrons are forced to make a circular motion by confining them in a

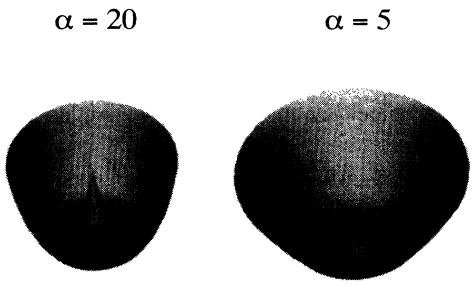

FIG. 1. The confinement potential $\alpha(1-r/r_0)^2$ with $r_0=10$ at $\alpha=5$ and 20. The parameter α, defined in Eq. (5), is inversely proportional to the width of the ring.

parabolic potential. The form of the confinement potentials which creates electron rings of various width are shown in Figs. 1 and 2. The model described below therefore describes rings of finite width which are closer to the real systems as compared to earlier studies by other authors which describe only ideally narrow rings.[38] The parameter α, which controls the width of the ring as seen in these figures, will be described below. In the following, we derive the essential formalism for single-electron and many-electron systems.

A. Single-electron system

The Hamiltonian for a particle confined to a circular motion by a parabolic potential and subject to a perpendicular magnetic field is given by

$$\mathcal{H}=\frac{1}{2m^*}\left[\mathbf{p}-\frac{e}{c}\mathbf{A}\right]^2+\tfrac{1}{2}m^*\omega_0^2(r-r_0)^2 . \tag{2}$$

In what follows, we choose the symmetric gauge vector potential $\mathbf{A}=\frac{1}{2}B(-y,x,0)$. In polar coordinates the Schrödinger equation then takes the form

$$-\frac{\hbar^2}{2m^*}\left\{\frac{\partial^2\psi}{\partial r^2}+\frac{1}{r}\frac{\partial\psi}{\partial r}+\frac{1}{r^2}\frac{\partial^2\psi}{\partial\theta^2}\right\}-\frac{ieB\hbar}{2m^*c}\frac{\partial\psi}{\partial\theta}+\left[\frac{e^2B^2r^2}{8m^*c^2}+\tfrac{1}{2}m^*\omega_0^2(r-r_0)^2-E\right]\psi=0 . \tag{3}$$

Introducing the ansatz

$$\psi=\frac{1}{\sqrt{2\pi}}f(r)e^{-il\theta} ,$$

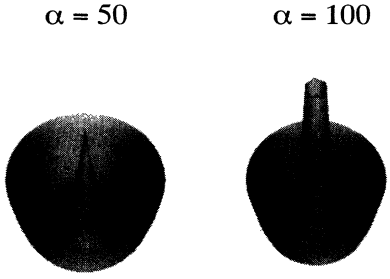

FIG. 2. Same as in Fig. 1, but for $\alpha=50$ and 100.

Eq. (3) can be easily separated, and the radial part is

$$-\frac{\hbar^2}{2m^*}\left\{\frac{d^2f}{dr^2}+\frac{1}{r}\frac{df}{dr}-\frac{l^2}{r^2}f\right\}-\frac{eB\hbar}{2m^*c}lf+\left[\frac{e^2B^2}{8m^*c^2}r^2+\tfrac{1}{2}m^*\omega_0^2(r-r_0)^2-E\right]f=0 . \tag{4}$$

Let us introduce the units

$$\mathcal{N}=\frac{BeA}{hc},\quad \alpha=\frac{\omega_0 m^* A}{h} , \tag{5}$$

where A is the area of the ring, i.e., $A=\pi r_0^2$. The various terms in the radial equation (4) can now be written as

$$\frac{eB\hbar}{2m^*c}=\frac{\hbar^2}{2m^*r_0^2}2\mathcal{N} ,$$

$$\frac{e^2B^2}{8m^*c^2}r^2=\frac{\hbar^2}{2m^*r_0^2}\mathcal{N}^2\left[\frac{r}{r_0}\right]^2 ,$$

$$\tfrac{1}{2}m^*\omega_0^2(r-r_0)^2=\frac{\hbar^2}{2m^*r_0^2}4\alpha^2\left[\frac{r}{r_0}-1\right]^2 ,$$

$$E=\frac{\hbar^2}{2m^*r_0^2}\frac{2m^*\pi A}{h^2}4\mathcal{E} .$$

Parameter α is inversely proportional to the width of the ring: as ω_0 is increased, the ring becomes narrower. Similarly, if the area is increased, then the relative width (with respect to the diameter) of the ring becomes smaller. As shown in the confinement potentials plotted in Figs. 1 and 2 [which, in fact, depict $\alpha(1-r/r_0)^2$ for various values of α], large α corresponds to a narrow path for the electrons to traverse and hence the electron motion is essentially in a strictly one-dimensional ring, whereas for small α the electron motion is almost two dimensional.

A brief note about how to convert the results presented below to more conventional units. First, one has to specify the radius of the ring, i.e., $R=r_0/10^{-9}$ m. Once that is fixed, the energy results obtained for that radius are multiplied by $(m_e/m^*)1/(152.4R^2)$ to obtain its value in meV. To obtain the magnetic field B in T, one should multiply $\mathcal{N}$ by $1/(1316\ R^2)$. The results for the confinement energy are $\hbar\omega_0=\alpha m_e/(152.4m^*R^2)$ in meV, where α is defined in (5).

If we now substitute the dimensionless quantities

$$x=\frac{r}{r_0},\quad \mathcal{E}=\frac{2m^*\pi A}{h^2}E , \tag{6}$$

the radial equation (4) takes the form

$$f''+\frac{1}{x}f'+\left[4\mathcal{E}+2\mathcal{N}l-4\alpha^2-(\mathcal{N}^2+4\alpha^2)x^2+8\alpha^2x-\frac{l^2}{x^2}\right]f=0 . \tag{7}$$

Let us first consider the case where the electron is confined to a one-dimensional circle. In our model, this corresponds to a δ-function confinement, i.e., $x=1$ is set

identically. Equation (7) then reduces to

$$[4\mathcal{E}+2\mathcal{N}l-4\alpha^2-(\mathcal{N}^2+4\alpha^2)+8\alpha^2-l^2]f=0 . \quad (8)$$

The solution of the equation is, as expected for an electron on a circular ring,[7,8,39,40]

$$\mathcal{E}=\tfrac{1}{4}(\mathcal{N}-l)^2 , \quad (9)$$

or, in a more familiar form in the original units,

$$E=\frac{\hbar^2}{2m^*r_0^2}\left[l-\frac{\Phi}{\Phi_0}\right]^2 .$$

We also consider the other limit, where the magnetic field is large compared to the confinement α. In this limit we have

$$f''+\frac{1}{x}f'+\left[4\mathcal{E}+2\mathcal{N}l-\mathcal{N}^2x^2-\frac{l^2}{x^2}\right]f=0 . \quad (10)$$

With the substitutions $u=x^{-1/2}f$ and $t=\mathcal{N}^{1/2}x$, Eq. (10) can further be written as

$$u''+\left[\frac{4\mathcal{E}+2\mathcal{N}l}{\mathcal{N}}-t^2+\frac{1-4l^2}{4t^2}\right]u=0 , \quad (11)$$

which is the familiar equation for Landau levels. The eigenvalues $\mathcal{E}$ are

$$\mathcal{E}=(n+\tfrac{1}{2})\mathcal{N} , \quad (12)$$

or, in the original units,

$$E=\hbar\omega_c(n+\tfrac{1}{2}) ,$$

where $\omega_c=Be/m^*c$ is the cyclotron frequency. Therefore, we recover the usual two-dimensional electron system in a magnetic field in the appropriate limit. In order to calculate the single-electron energy levels, we have solved Eq. (7) numerically for various values of α, and the results are presented in Fig. 3. As expected, for large values of α ($\alpha\geq 20$), in the low-energy range the energy spectrum is close to that of an ideally narrow ring [Eq. (9)] and is given by a set of translated parabolas. The upper Landau band remains at much higher energies. As the value of α is decreased, the upper Landau band comes down in energy and the Landau levels begin to form even at very low values of Φ/Φ_0. The level crossings are also quite prevalent in the case of $\alpha=5$, as shown in Fig. 3.

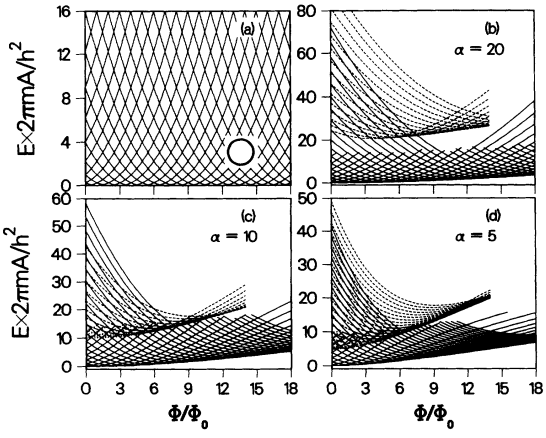

FIG. 3. Single-electron energy levels as a function of the magnetic field for (a) a narrow ring and (b)–(d) parabolic confinement model with various values of confinement potential strength. The second Fock-Darwin level is potted as dotted lines.

B. Interaction matrix elements

Since single-electron wave functions are obtained numerically, we need to derive an expression for the interaction matrix element which is suitable for our numerical work. We begin by writing the interaction potential as the Fourier transform integral:

$$V(\mathbf{r})=\frac{1}{(2\pi)^2}\int V(\mathbf{q})e^{-i\mathbf{q}\cdot\mathbf{r}}d\mathbf{q} .$$

Single-electron wave functions are also written in the similar fashion:

$$\psi_\lambda(\mathbf{r})=\frac{1}{(2\pi)^2}\int \phi_\lambda(\mathbf{q})e^{-i\mathbf{q}\cdot\mathbf{r}}d\mathbf{q} .$$

The two-body matrix element

$$V_{\lambda_1\lambda_2\lambda_3\lambda_4}=\int \psi^*_{\lambda_1}(\mathbf{r}_1)\psi^*_{\lambda_2}(\mathbf{r}_2)V(\mathbf{r}_1-\mathbf{r}_2)\times\psi_{\lambda_3}(\mathbf{r}_2)\psi_{\lambda_4}(\mathbf{r}_1)d\mathbf{r}_1d\mathbf{r}_2 \quad (13)$$

can then be written as

$$V_{\lambda_1\lambda_2\lambda_3\lambda_4}=\frac{1}{(2\pi)^6}\int \phi^*_{\lambda_1}(\mathbf{q}_1)\phi_{\lambda_4}(\mathbf{q}_1-\mathbf{q})\phi^*_{\lambda_2}(\mathbf{q}_2)\times\phi_{\lambda_3}(\mathbf{q}_2+\mathbf{q})V(\mathbf{q})d\mathbf{q}_1d\mathbf{q}_2d\mathbf{q} . \quad (14)$$

The convolution integrals appearing in Eq. (14) are most conveniently evaluated in $\mathbf{r}$ space in the following manner:

$$C_{\lambda\lambda'}(\mathbf{q})=\int \phi^*_\lambda(\mathbf{k})\phi_{\lambda'}(\mathbf{k}-\mathbf{q})d\mathbf{k}=(2\pi)^2\int \psi^*_\lambda(\mathbf{r})\psi_{\lambda'}(\mathbf{r})e^{-i\mathbf{q}\cdot\mathbf{r}}d\mathbf{r} \quad (15)$$

and

$$D_{\lambda\lambda'}(\mathbf{q})=\int \phi^*_\lambda(\mathbf{k})\phi_{\lambda'}(\mathbf{k}+\mathbf{q})d\mathbf{k}=(2\pi)^2\int \psi^*_\lambda(\mathbf{r})\psi_{\lambda'}(\mathbf{r})e^{i\mathbf{q}\cdot\mathbf{r}}d\mathbf{r}=C_{\lambda\lambda'}(-\mathbf{q}) . \quad (16)$$

With these notations the interaction matrix element takes the form

$$V_{\lambda_1\lambda_2\lambda_3\lambda_4}=\frac{1}{(2\pi)^2}\int C_{\lambda_1\lambda_4}(\mathbf{q})D_{\lambda_2\lambda_3}(\mathbf{q})V(\mathbf{q})d\mathbf{q} . \quad (17)$$

In a quantum ring, or in any cylindrically symmetric system, the wave functions are of the form

$$\psi_\lambda(\mathbf{r})=R_{nl}(r)e^{il\theta},\quad l=0,\pm1,\pm2,\ldots , \quad (18)$$

where λ represents the quantum number pair $\{n,l\}$. Substituting this particular form of the wave function to the convolution integral (15) and denoting by m the difference $(l-l')$ and by θ_q the angle between $\mathbf{q}$ and the

x axis, we obtain

$$C_{\lambda\lambda'}(\mathbf{q})=\int R_{nl}(r)R_{n'l'}(r)e^{i(l-l')\theta}e^{-i\mathbf{q}\cdot\mathbf{r}}d\mathbf{r}$$
$$=\int R_{nl}(r)R_{n'l'}(r)e^{im\theta}e^{-iqr\cos(\theta_q-\theta)}r\,dr\,d\theta$$
$$=2\pi i^{-m}(-1)^m e^{im\theta_q}\int_0^\infty J_m(qr)R_{nl}(r)R_{n'l'}(r)r\,dr\ . \tag{19}$$

Here J_m is Bessel's function of order m. The other convolution integral (16) can also be evaluated similarly to give

$$D_{\lambda\lambda'}(\mathbf{q})=2\pi i^{-m}e^{im\theta_q}\int_0^\infty J_m(qr)R_{nl}(r)R_{n'l'}(r)r\,dr\ . \tag{20}$$

Substituting these into the matrix element (17) and making use of the symmetry relation $J_{-m}=(-1)^m J_m$, the interaction matrix elements can be expressed as

$$V_{\lambda_1\lambda_2\lambda_3\lambda_4}=\delta_{l_1+l_2,l_3+l_4}2\pi\int_0^\infty dq\,qV(q)\int_0^\infty dr_1 r_1 J_{|l_1-l_4|}(qr_1)R_{n_1l_1}(r_1)R_{n_4l_4}(r_1)$$
$$\times\int_0^\infty dr_2 r_2 J_{|l_2-l_3|}(qr_2)R_{n_2l_2}(r_2)R_{n_3l_3}(r_2)\ . \tag{21}$$

In principle this form could be used to evaluate the interaction matrix elements. In the present case, however, we have no analytic expression for the radial wave functions R_n. This means that the integer Bessel transforms of Eq. (21) should be computed numerically. Let us now consider the Coulombic interaction in a plane, i.e., take the form of interaction potential to be $V(\mathbf{r})=\beta/r$, so that the Fourier transform is $V(\mathbf{q})=2\pi\beta/q$. In that case, the integration over q in Eq. (21) can be evaluated to be

$$\int_0^\infty J_m(qr_1)J_m(qr_2)dq=\frac{r_2^m}{r_1^{m+1}}\frac{\Gamma(m+\frac{1}{2})}{\Gamma(m+1)\Gamma(\frac{1}{2})}\mathcal{F}\left[m+\tfrac{1}{2},\tfrac{1}{2};m+1\left[\frac{r_2}{r_1}\right]^2\right],\quad r_2<r_1\ . \tag{22}$$

Here $\mathcal{F}$ is the Gauss hypergeometric function. When $r_2>r_1$, the result is the same except that the roles of r_1 and r_2 are interchanged. The hypergeometric function can be evaluated from its power series. For that purpose let us denote by M_m the series

$$M_m(z)=\sum_{n=0}Q_n^{(m)}z^n\ , \tag{23}$$

where the coefficients $Q_n^{(m)}$ are defined recursively as

$$Q_0^{(0)}=1\ ,$$
$$Q_0^{(m+1)}=\frac{m+\frac{1}{2}}{m+1}Q_0^{(m)}\ , \tag{24}$$
$$Q_{n+1}^{(m)}=\frac{(m+\frac{1}{2}+n)(\frac{1}{2}+n)}{(m+1+n)(n+1)}Q_n^{(m)}\ .$$

Integral (22) then evaluated to be

$$\int_0^\infty J_m(qr_1)J_m(qr_2)dq=\frac{r_2^m}{r_1^{m+1}}M_m\left[\frac{r_2^2}{r_1^2}\right],\quad r_2<r_1$$

and, similarly, the matrix element (21):

$$V_{\lambda_1\lambda_2\lambda_3\lambda_4}=(2\pi)^2\beta\delta_{l_1+l_2,l_3+l_4}$$
$$\times\left\{\int_0^\infty dr_1 R_{n_1l_1}(r_1)R_{n_4l_4}(r_1)\frac{1}{r_1^m}\int_0^{r_1}dr_2 R_{n_2l_2}(r_2)R_{n_3l_3}(r_2)r_2^{|l_2+l_3|+1}M_{|l_2-l_3|}\left[\frac{r_2^2}{r_1^2}\right]\right.$$
$$\left.+\int_0^\infty dr_2 R_{n_2l_2}(r_2)R_{n_3l_3}(r_2)\frac{1}{r_2^m}\int_0^{r_2}dr_1 R_{n_1l_1}(r_1)R_{n_4l_4}(r_1)r_1^{|l_1-l_4|+1}M_{|l_1-l_4|}\left[\frac{r_1^2}{r_2^2}\right]\right\}\ . \tag{25}$$

This is the form of interaction matrix elements used to obtain the numerical results presented below. As mentioned above, we have used the Coulomb interaction in a plane: $V(q)=2\pi\kappa/q$, where $\kappa=e^2/4\pi\epsilon_0\epsilon$, and in the numerical calculations that follow we have used the values $m^*=0.07m$, $\epsilon=13$, and the radius of the ring $r_0=10$ nm.

C. Magnetization

Experimentally, one measures the magnetization which arises due to the persistent current in single, isolated loops.[1–3] In our present work, the magnetic moment is calculated from its thermodynamic expression

$$\mathcal{M}=-\sum_m \frac{\partial E_m}{\partial B} e^{-E_m/kT} \Big/ \sum_m e^{-E_m/kT} . \tag{26}$$

The partial derivatives $\partial E_m/\partial B$ were evaluated as the expectation values of the magnetization operator in the interacting states $|m\rangle$. In the ring geometry (i.e., in the symmetric gauge), the magnetization operator takes the form[40]

$$M=\frac{\partial \mathcal{H}}{\partial B} = \frac{1}{2m^*}\left[\frac{e}{c}L_z+\frac{e^2B}{2c^2}r^2\right] . \tag{27}$$

The magnetization $\mathcal{M}$ (in units of energy $/\mathcal{N}$) and susceptibility are periodic functions[35] which are gradually damped with decreasing α at high fields, reflecting the behavior of the energy levels.

To guarantee the convergence of the sum in (26) one has to go to high enough energies E_m of the interacting many-particle system, and to obtain energies E_m accurately enough one must include a large number of single-particle states to build up the noninteracting many-particle basis states. Furthermore, to track the behavior of the magnetic moment as a function of the applied magnetic field, a considerable range in magnetic field (B) has to be spanned. This implies that one must have a huge number of single-particle wave functions available. To help the resulting bookkeeping problems and speed up the calculations, the numerical solutions of the single-particle equation (7) were stored into a data base. This data base was consulted during the formation of the Hamiltonian matrix, and dynamically updated in the case where no matching wave function was found. The Hamiltonian consists of matrix elements of the operator (2) between noninteracting many-particle states, i.e., essentially of the superpositions of the Coulomb terms (21). In fact, a vast number of terms (21) is required for the construction of the Hamiltonian. On the other hand, the same elements are repeatedly used in the Hamiltonian, though they differ in the number of particles or in the total angular momentum. We therefore put the elements $V_{\lambda_1,\lambda_2,\lambda_3,\lambda_4}$ into a dynamic data base, where they can be retrieved when needed.

III. RESULTS AND DISCUSSION

As mentioned in Sec. I, we restrict ourselves in this paper only to impurity-free systems. For reasons to be explained below, few-electron systems and somewhat larger systems display significantly different results, and below we present a detailed analysis of these two cases.

A. Few-electron systems

In Fig. 4 we show the energies, and in Fig. 5 the magnetic moments of four interacting and noninteracting electrons at $\alpha=20$ and 5. It is clear that the only discernible effect of the Coulomb interaction is to shift the noninteracting energy spectrum to higher values of energy. This is due to the fact that in the lowest Landau level

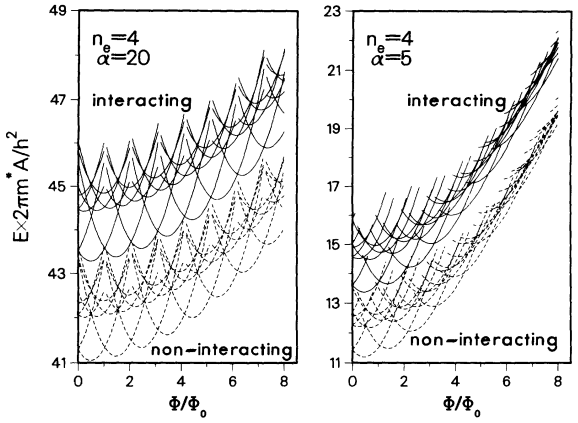

FIG. 4. Energy spectrum for the four interacting (solid lines) and noninteracting (dashed lines) electron systems at $\alpha=20$ and 5 for several values of temperature T (in units of energy).

all close-lying states belong to different angular momentum, and Coulomb interaction cannot couple them because of the conservation of the angular momentum. The excited states seem to be shifted from the ground state somewhat more than the corresponding noninteracting values. At $\alpha=20$, the interaction has practically no effect on the magnetization, which is, as expected, a periodic function with period Φ_0. At $\alpha=5$, the magnetization is a sharp periodic function for small magnetic fields and is then rapidly damped as the Landau levels begin to form. There is a a slight shift in phase between noninteracting and interacting system results.

The situation remains the same for the five-electron system, as shown in Figs. 6 and 7, where we present the energies and magnetization, respectively. The energy shift due to the Coulomb interaction is slightly more pronounced in this case. The magnetization result is also similar to that of the four-electron system, except that the oscillations of the magnetization curves have opposite phases for odd and even numbers of electrons. This can readily be explained in terms of the occupation of an even

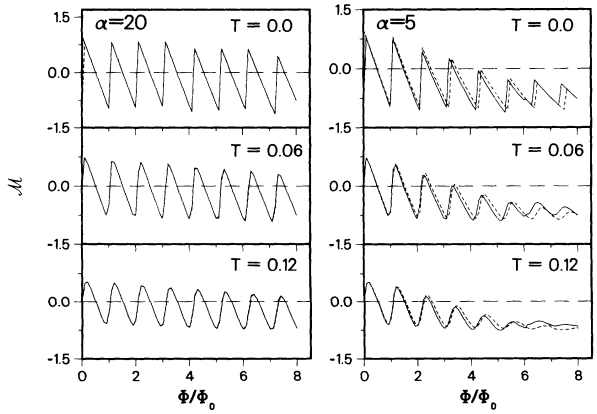

FIG. 5. Magnetization for the four-electron system and for the parameters as in Fig. 4. At $\alpha=20$ the magnetic moments for the interacting and noninteracting systems are identical.

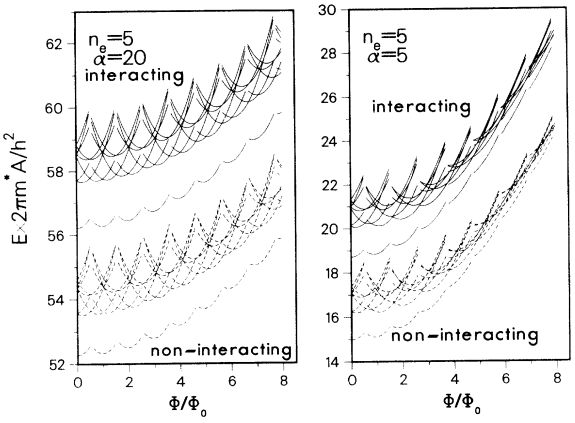

FIG. 6. Same as in Fig. 4 but for a five-electron system.

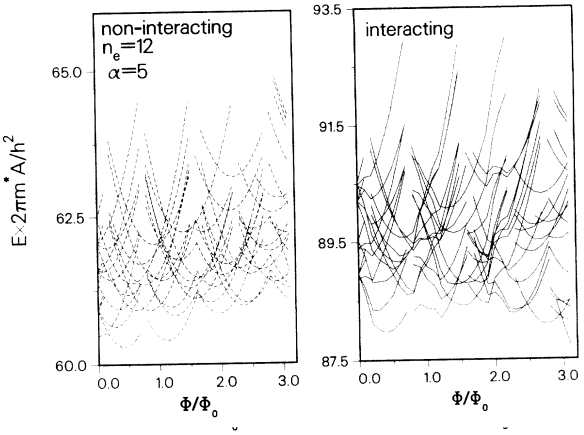

FIG. 8. Energy spectrum (qualitative) for a 12-electron system at $\alpha=5$.

or odd number of single-electron levels. These results are therefore in sharp contrast to those of a quantum dot, where the Coulomb interaction has important effects on the energy spectrum[26] and introduces structures in the magnetization.[30] It is interesting to note that several authors[41] have either conjectured or found in their model systems that for a fairly weak form of Coulomb interaction the persistent current in a one-dimensional ring is independent of the presence and/or strength of the Coulomb interaction. The results of our present method (see also Ref. 34) are, of course, independent confirmation of those assertions in a much more general case.

B. Many-electron systems

The energy results presented above indicate that at degenerate points the energy curves have slopes of opposite sign. This means that the magnetization practically vanishes at these points. On the other hand, in the upper Landau band there may be intersections where slopes have the same sign. This would imply a dramatic increase in magnetization. Coulomb interaction can in fact couple states better in the second Landau band than in the lowest Landau band. Therefore, we have also estimated the effects of the Coulomb interaction in the case where the electrons occupy single-particle levels in the second Landau level. This (multiple-subband occupation) is to be contrasted with the case when the electrons in the noninteracting ground state occupy only a few of the lowest single-electron levels in the first subband. There, in general, the excited states with the angular momentum of the ground state are energetically so high that the Coulomb interaction cannot mix them into the interacting ground state. It is clear that the density of the noninteracting many-particle levels will increase with the number of electrons. This is especially so when in a configuration there are particles with different values of the principal quantum number because it is then possible to form configurations with almost the same energy that still preserves the total angular momentum. This implies that the Coulomb force can easily mix these configurations. Unfortunately the resulting high density of states and the number of particles involved makes this system very difficult for numerical studies.

To obtain qualitative estimates for the behavior of many-particle systems we have to limit drastically the number of states in the noninteracting basis: we included all states whose energy was less than the energy of the configuration where m lowest-lying particles were excited just above the Fermi level, and restricted the number of unoccupied states, m, to 2, or 3. As an example we have

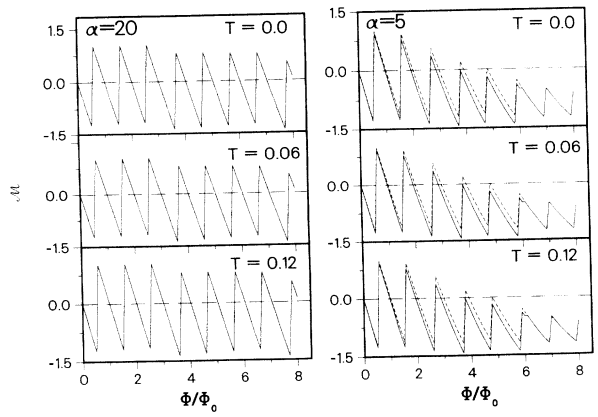

FIG. 7. Same as in Fig. 5 but for a five-electron system.

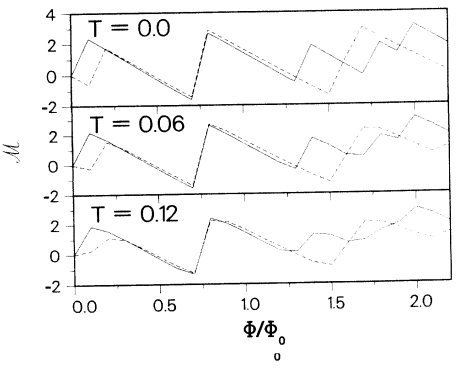

FIG. 9. Magnetization for a 12-electron system at $\alpha=5$ derived from the energies shown in Fig. 8.

studied 12 electrons in a ring with confinement $\alpha=5$ (Figs. 8 and 9). At low values of the magnetic field this system has two electrons in the second Landau level. Numerical studies show that at certain values of the magnetic field some states with different angular momenta tend to group together to form a nearly degenerate ground state. The grouping occurs at points where the states involved have, as a function of the magnetic field, slopes of the same sign (Fig. 8). Because the magnetization is proportional to the derivative of the energy with respect to the magnetic field, this grouping would cause a dramatic increase in the magnetization (Fig. 9).

IV. SUMMARY

We have investigated eigenstates of a few interacting and noninteracting electrons in a quantum ring, subjected to a perpendicular magnetic field. In contrast to the standard perturbative approaches used earlier by several authors, we have studied the interacting electron states by directly solving the many-electron problem numerically. We have made a connection with earlier work[7,8] for a single electron by studying various limiting cases: the ideally narrow ring and the usual two-dimensional electron gas. This shows the general character of our model. We find that in the lowest Landau level the Coulomb interaction is found simply to shift upward the energy spectrum of the noninteracting system. For a ring close to being ideally narrow, originally studied in Refs. 7 and 8, there is no discernible effect of the interaction on the magnetization. The reason lies in the conservation of the angular momentum: all close-lying states in the lowest Landau band belong to different angular momentum, and the Coulomb force cannot couple them. Our qualitative estimates indicate that if there are so many electrons in the system that the second Landau band begins to be occupied, then the density of the noninteracting levels is very high. There are then many levels with the same angular momentum very close to each other so that the Coulomb force can couple them. The result is a rapid increase in the magnetization. The circular symmetry in the lowest Landau level can, however, be broken by adding an impurity in the ring, which might generate a far more active role for the electron-electron interactions than what is observed here. In our present model, we can also include the electron-spin degrees of freedom. In these cases, of course, the computations are much more involved. It should also be stressed that the field of quantum confinement has achieved great advancement in recent years. In addition to the energy levels described above, a measurement of even the pair-correlation functions of quantum rings will perhaps be possible in quantum rings created in the fashion of "quantum corrals."[42] These will be the subject of our future publications.

ACKNOWLEDGMENTS

The initial part of the work was done by one of us (T.C.) while at the National Research Council of Canada, Ottawa. He wishes to thank Geof Aers in the theory group, for helpful discussions.

*Electronic address: tapash@imsc.ernet.in
†Electronic address: ppi@eero.oulu.fi

[1]L. P. Levy, G. Dolan, J. Dunsmuir, and H. Bouchiat, Phys. Rev. Lett. **64**, 2074 (1990).
[2]V. Chandrasekhar, R. A. Webb, M. J. Brady, M. B. Ketchen, W. J. Gallagher, and A. Kleinsasser, Phys. Rev. Lett. **67**, 3578 (1991).
[3]D. Mailly, C. Chapelier, and A. Benoit, Phys. Rev. Lett. **70**, 2020 (1993).
[4]Y. Aharonov and D. Bohm, Phys. Rev. **115**, 485 (1959).
[5]It has been pointed out recently [A. Müller-Groeling and H. A. Weidenmüller, Phys. Rev. B **49**, 4752 (1994)] that the existence of the persistent current was first predicted in F. Hund, Ann. Phys. (Leipzig) **32**, 102 (1938).
[6]N. Byers and C. N. Yang, Phys. Rev. Lett. **7**, 46 (1961); F. Bloch, Phys. Rev. B **2**, 109 (1970).
[7]Y. Imry, in *Quantum Coherences in Mesoscopic Systems,* edited by B. Kramer (Plenum, New York, 1991), p. 221.
[8]M. Büttiker, Y. Imry, and R. Landauer, Phys. Lett. A **96**, 365 (1983).
[9]H. F. Cheung, Y. Gefen, E. K. Riedel, and W. H. Shih, Phys. Rev. B **37**, 6050 (1988); H. F. Cheung, Y. Gefen, and E. K. Riedel, IBM J. Res. Dev. **32**, 359 (1988).
[10]R. B. Laughlin, Phys. Rev. B **23**, 5632 (1981); see also, Y. Imry, J. Phys. C **16**, 3501 (1983).
[11]B. I. Halperin, Phys. Rev. B **25**, 2185 (1982).
[12]T. Chakraborty, in *Handbook on Semiconductors,* edited by P. T. Landsberg (North-Holland, Amsterdam, 1992), Vol. 1. Chap. 17; T. Chakraborty and P. Pietiläinen, *The Fractional Quantum Hall Effect* (Springer-Verlag, New York, 1988).
[13]A. Benoit, D. Mailly, M. El-Khatib, and P. Perrier, in Ref. 6, p. 237.
[14]U. Sivan and Y. Imry, Phys. Rev. Lett **61**, 1001 (1988).
[15]E. N. Bogacheck and G. A. Gogadze, Zh. Eksp. Teor. Fiz. **63**, 1839 (1972) [Sov. Phys. JETP **36**, 973 (1973)]; N. B. Brandt *et al., ibid.* **72**, 2332 (1977) [*ibid.* **45**, 1226 (1977)].
[16]D. Wohlleben *et al.*, Phys. Rev. Lett. **66**, 3191 (1991).
[17]S. Iijima, Nature (London) **354**, 56 (1991).
[18]H. Ajiki and T. Ando, J. Phys. Soc. Jpn. **62**, 2470 (1993).
[19]T. Chakraborty, Comments Condens. Matter Phys. **16**, 35 (1992).
[20]D. Heitmann and J. P. Kotthaus, Phys. Today **46** (6), 56 (1993); M. A. Reed, Sci. Am. **268**, 118 (1993).
[21]*Transport Phenomena in Mesoscopic Systems,* edited by H. Fukuyama and T. Ando (Springer-Verlag, Heidelberg, 1992).
[22]T. Demel, D. Heitmann, P. Grambow, and K. Ploog, Phys. Rev. Lett. **64**, 788 (1990); Ch. Sikorski and U. Merkt, *ibid.* **62**, 2164 (1989).
[23]P. L. McEuen *et al.*, Phys. Rev. Lett. **66**, 1926 (1991).
[24]L. P. Kouwenhoven, B. J. van Wees, C. J. P. Harmans, and J. G. Williamson, Surf. Sci. **229**, 290 (1990); A. T. Johnson *et al.*, Phys. Rev. Lett. **69**, 592 (1992).
[25]C. W. J. Beenakker, H. van Houten, and A. A. M. Staring, Phys. Rev. B **44**, 1657 (1991); see also H. van Houten, C. W. J. Beenakker, and A. A. M. Staring, in *Single Charge Tunneling,* edited by H. Grabert and M. H. Devoret (Plenum, New

York, 1991), p. 167.
[26]P. A. Maksym and T. Chakraborty, Phys. Rev. Lett. **65**, 108 (1990).
[27]R. C. Ashoori, H. L. Stormer, J. S. Weiner, L. N. Pfeiffer, K. W. Baldwin, and K. W. West, Phys. Rev. Lett. **71**, 613 (1993).
[28]The experimental results have been recently reinterpreted as due to the Coulomb interaction effect; see P. L. McEuen *et al.*, Phys. Rev. B **45**, 11 419 (1992).
[29]V. Fock, Z. Phys. **47**, 446 (1928); C. G. Darwin, Proc. Cambridge Philos. Soc. **27**, 86 (1930).
[30]P. A. Maksym and T. Chakraborty, Phys. Rev. B **45**, 1947 (1992).
[31]M. Wagner, U. Merkt, and A. V. Chaplik, Phys. Rev. B **45**, 1951 (1992).
[32]V. Ambegaokar and U. Eckern, Phys. Rev. Lett. **65**, 381 (1990); see also B. L. Altshuler, D. E. Khmel'nitzkii, and B. Z. Spivak, Solid State Commun. **48**, 10 (1983).
[33]U. Eckern and A. Schmid, Europhys. Lett. **18**, 457 (1992).
[34]A brief description of the work has been published in P. Pietiläinen and T. Chakraborty, Solid State Commun. **87**, 809 (1993).
[35]T. Chakraborty and P. Pietiläinen, in *Transport Phenomena in Mesoscopic Systems* (Ref. 21).
[36]B. Meurer, D. Heitmann, and K. Ploog, Phys. Rev. Lett. **68**, 1371 (1992).
[37]L. J. Challis, Contemp. Phys. **33**, 111 (1992).
[38]The importance of the finite width of the mesoscopic ring when comparing the existing theories with experimental results was recognized by A. Groshev, I. Z. Kostadinov, and I. Dobrianov, Phys. Rev. B **45**, 6279 (1992). However, they used the conventional approach (Refs. 7–9) and did not include electron correlations.
[39]D. Loss and P. Goldbart, Phys. Rev. B **43**, 13 762 (1991).
[40]R. L. Schult, M. Stone, H. W. Wyld, and D. G. Ravenhall, Superlatt. Microstruct. **11**, 73 (1992).
[41]A. J. Leggett, in *Granular Nanoelectronics,* edited by D. K. Ferry, J. R. Berker, and C. Jacoboni, Vol. 251 of *NATO Advanced Study Institute, Series B: Physics* (Plenum, New York, 1992), p. 297; D. Loss, Phys. Rev. Lett. **69**, 343 (1992); A. Müller-Groeling and H. A. Weidenmüller, Phys. Rev. B **49**, 4752 (1994).
[42]M. F. Crommie, C. P. Lutz, and D. M. Eigler, Science **262**, 218 (1993).

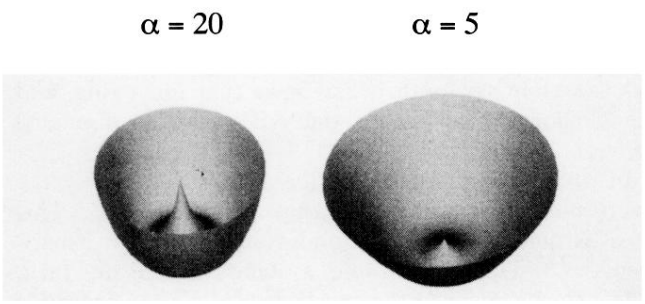

FIG. 1. The confinement potential $\alpha(1-r/r_0)^2$ with $r_0=10$ at $\alpha=5$ and 20. The parameter α, defined in Eq. (5), is inversely proportional to the width of the ring.

$\alpha = 50$ $\alpha = 100$

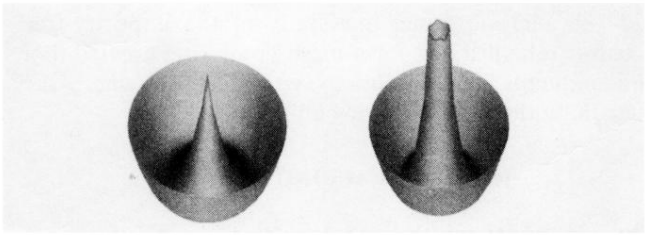

FIG. 2. Same as in Fig. 1, but for $\alpha = 50$ and 100.